Vol 16 No 3, March 2007
1009-1963/2007/16(03)/0758-08

Chinese Physics

© 2007 Chin. Phys. Soc.
and IOP Publishing Ltd

Review of relaxation oscillations in plasma processing discharges*

Zhou Zhu-Wen(周筑文)[a)†], M. A. Lieberman[b)], and Sungjin Kim[b)]

[a)] *Department of Physics, Guizhou Educational College, Guiyang* 550003, *China*
[b)] *Department of Electrical Engineering and Computer Sciences-* 1770 *University of California, Berkeley, CA* 94720, *U.S.A.*

(Received 28 May 2006; revised manuscript received 12 September 2006)

Relaxation oscillations due to plasma instabilities at frequencies ranging from a few Hz to tens of kHz have been observed in various types of plasma processing discharges. Relaxation oscillations have been observed in electropositive capacitive discharges between a powered anode and a metallic chamber whose periphery is grounded through a slot with dielectric spacers. The oscillations of time-varying optical emission from the main discharge chamber show, for example, a high-frequency ($\sim$ 40 kHz) relaxation oscillation at 13.33Pa, with an absorbed power being nearly the peripheral breakdown power, and a low-frequency ($\sim$ 3 Hz) oscillation, with an even higher absorbed power. The high-frequency oscillation is found to ignite plasma in the slot, but usually not in the peripheral chamber. The kilohertz oscillations are modelled using an electromagnetic model of the slot impedance, coupled to a circuit analysis of the system including the matching network. The model results are in general agreement with the experimental observations, and indicate a variety of behaviours dependent on the matching conditions. In low-pressure inductive discharges, oscillations appear in the transition between low-density capacitively driven and high-density inductively driven discharges when attaching gases such as SF_6 and Ar/SF_6 mixtures are used. Oscillations of charged particles, plasma potential, and light, at frequencies ranging from a few Hz to tens of kHz, are seen for gas pressures between 0.133 Pa and 13.33 Pa and discharge powers in a range of 75–1200 W. The region of instability increases as the plasma becomes more electronegative, and the frequency of plasma oscillation increases as the power, pressure, and gas flow rate increase. A volume-averaged (global) model of the kilohertz instability has been developed; the results obtained from the model agree well with the experimental observations.

Keywords: relaxation oscillation, capacitive discharges, inductive discharges, plasma instability
PACC: 5235, 5235P

1. Introduction

Plasma instabilities in capacitively and inductively coupled radio-frequency (rf) plasmas have been studied both experimentally and theoretically in the last few years.[1−9] Low-pressure rf plasma sources have been increasingly used for industrial material processes such as etching and deposition.[10] Their simple design with no external magnetic field and their ability to produce high-density plasma have attracted the attention of many plasma equipment manufacturers. A particular capacitive configuration, which has been found to have desirable processing applications[11] and is shown schematically in Fig.1, is a dual-frequency capacitive discharge, with the main cylindrical discharge connected to a peripheral cylindrical (pumping) region through an annular slot narrowed with a dielectric. The feedstock gas flows from the main discharge region through the slot, and then it is pumped out in the grounded peripheral chamber. In the operation of a commercial reactor, instabilities and oscillations are sometimes observed, which produce detrimental effects on the processing.

As shown in the figure, the discharge is driven by a high frequency source with a frequency ω and voltage $V_{\rm rf}$ in series with a low frequency source with a frequency $\omega_{\rm b}$ and voltage $V_{\rm bias}$ that is taken as zero for the instability studies. The main discharge having a plate separation l is connected to a peripheral region with a length w and gap spacing g. The variable-gap slot is a flexible way of balancing the required pumping speed with confinement of plasma to the central region. Because of the small pumping conductance of the slot, there can exist a significant pressure gradient within the slot, which can be modelled by using different average pressures in the slot and peripheral

*Project supported by the National Science Foundation of USA (Grant No ECS-0139956).
†E-mail: zhuwenz@gmail.com

regions. The configuration in the figure is based on a commercial reactor, but the particular dimensions used are related to a research experiment that is purposely built to study some specific phenomena.

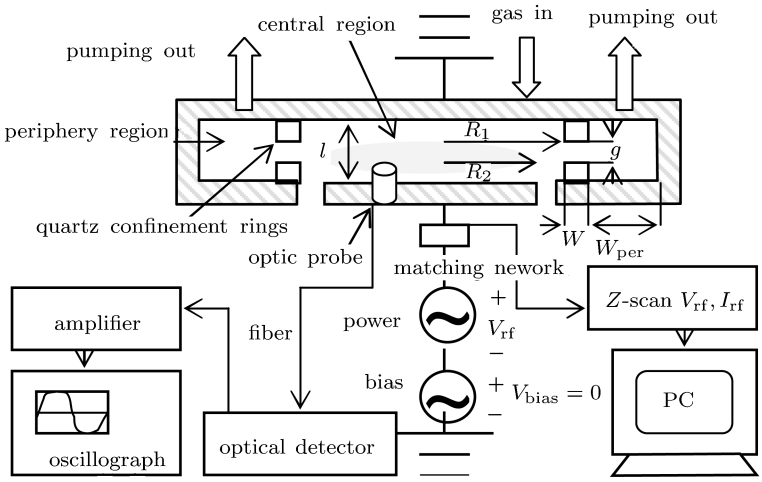


Fig.1. Schematic of the experimental capacitive discharge setup.

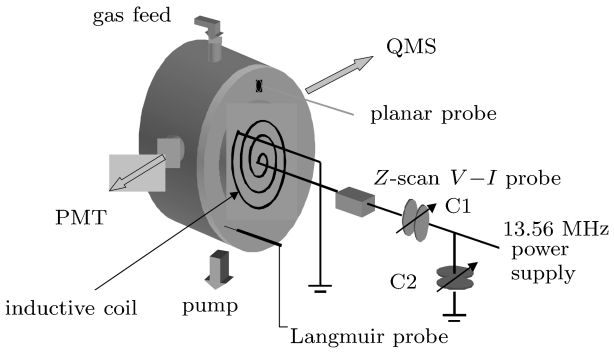


Fig.2. Schematic of the experimental inductive discharge setup.

In an inductive source, plasma is created by application of an rf power to a nonresonant inductive coil (see Fig.2), resulting in the breakdown of the working gas near the coil by the induced rf electric field. In most inductive discharges, the rf power is transferred to the plasma via both capacitive and inductive coupling.[12] At low input powers, the discharge is in a low-density capacitive mode (E mode) where the plasma is maintained by the electrostatic field of the inductive coil. For electropositive plasmas (no negative ions) as the input power gradually increases, a switch to inductive coupling occurs and the discharge has a rapid transition into a high-density inductive mode (H mode) where the plasma is sustained by the azimuthal electric field induced by the coil current. During this transition from capacitive to inductive modes, the jumps in plasma density and intensity of light emitted from the plasma can reach 1–2 orders of magnitude higher. Usually, the E- to H-mode transition exhibits hysteresis.[13] When electronegative gases (i.e. gases in which an electron attachment leads to the formation of negative ions) such as sulfur hexafluoride or oxygen are used, the transition between capacitive and inductive modes may exhibit unstable behaviour with oscillations of ion and electron densities, and of plasma potential.[3–9]

In Section 2, we describe the relaxation oscillations observed in the capacitive discharge configuration. In Section 3, we describe the oscillations seen in the inductive configuration. Conclusions and further discussion are given in Section 4.

2. Oscillations in capacitive reactors

The experiment,[1,2] sketched in Fig.1, is a dual-frequency capacitive discharge, with the main discharge connected to a peripheral (pumping) chamber through an annular quartz slot. The feedstock argon gas flows from the main discharge chamber through the slot, and is pumped in the grounded peripheral chamber. The discharge is driven by a high-frequency

source with a frequency $f_{\rm rf} = 27.1$ MHz and variable voltage $V_{\rm rf}$ in series with a low-frequency source with a variable voltage $V_{\rm bias}$. A single high-frequency ($V_{\rm bias} = 0$) is used. The main discharge, having a plate separation l, is connected to a peripheral region with a width $w_{\rm per}$ through an annular dielectric slot with a gap width w and gap spacing g. The configuration in the figure is based on a commercial reactor, but the particular experimental dimensions used to study the oscillations are $l = 2.54$ cm, $g = 0.635$ cm, $w = 3.8$ cm and $w_{\rm per} = 5.1$ cm. The powered electrode has R_2= 6.35 cm and central ground has $R_1 = 8.9$ cm.

Choosing a different confinement ring thickness, the gap spacing g can be varied, so that the effect of varying gap spacing on the plasma transport in the slot, and the slot and edge plasmas' breakdown and maintenance, can be measured and compared with the model. However, only the gap spacing given above is used for the instability studies. Other specifications are as follows: a stainless steel chamber body and electrode, a Z-scan RF measurement system, and an L-type matching network consisting of two vacuum Jenning capacitors with adjustable ranges being 12–500 pF and 12–1000 pF, a capacitance-fixed capacitor (1600 pF) and a 5μH inductor. Optical emission is observed with a 6 mm wide optical slot located on the ground electrode with a quartz cover plate, to obtain the radial variation of optical emission from the main discharge chamber, slot and periphery, along the entire diameter of the ground electrode. Other view ports are located at both ends of the two side extensions for the vacuum pump connection to provide a side angle view into the peripheral region and the slot between the confinement rings. Langmuir probes are used for density measurements in the central region and the periphery, and a floating potential ring in the central region is used to measure plasma potential.

In Figs.3 and 4, two types of relaxation oscillations are shown that occur in the capacitive discharge. Optical emission is observed in the 6 mm wide optical slot located on the ground electrode. In the figures I is the relative optical emission intensity in the main discharge region and peripheral region. In Fig.3 a high-frequency relaxation oscillation of 75.47 kHz is observed at 13.33 Pa and 8 W of absorbed power. The argon emission at 748.7 nm is detected through a notch filter and a fibre optic cable; and plasma potential V_p is also shown in the same figure. In Fig.4 the time-varying optical emission from the main discharge shows a low-frequency (2.72 Hz) relaxation oscillation at 13.33 Pa and 325 W of absorbed power. The optical emission intensity is a function of density and temperature as shown below.

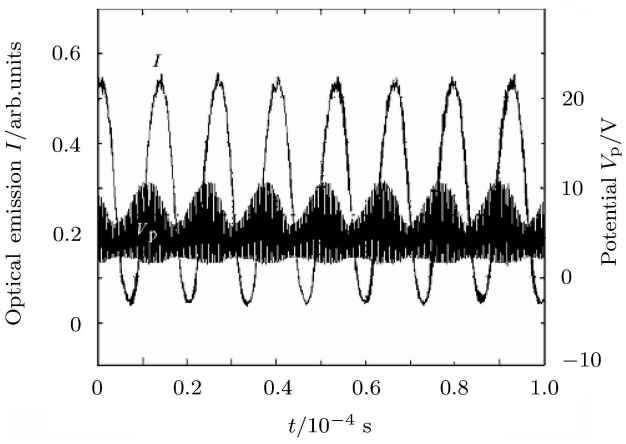


Fig.3. Time-varying optical emission I and plasma potential $V_{\rm p}$ from the main discharge region at 13.33 Pa and 8 W of absorbed power, showing a high-frequency (75.37 kHz) relaxation oscillation. Argon emission at 748.7 nm is detected through a notch filter and a fibre optic cable.

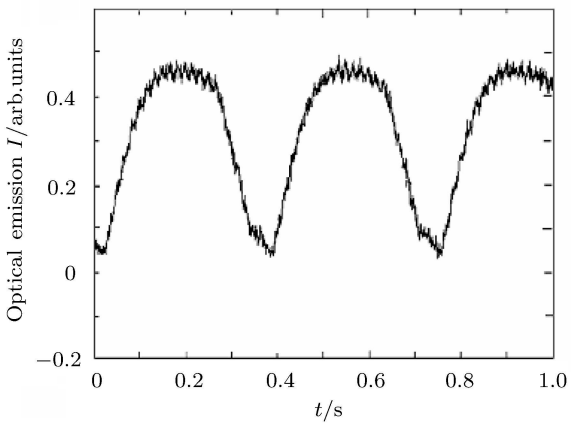


Fig.4. Time-varying optical emission I from the periphery region at 13.33 Pa and 325 W of absorbed power, showing a low-frequency (2.72 Hz) relaxation oscillation.

The rf voltage $\tilde{V}_{\rm rf}$ on the powered electrode just prior to loss of confinement is measured. The rf voltage $\tilde{V}_{\rm d}$ of the main discharge plasma with respect to ground is then determined using the scaling[12]

$$(\tilde{V}_{\rm rf} - \tilde{V}_{\rm d})/\tilde{V}_{\rm d} \propto (A_{\rm gnd}/A_{\rm pow})^{2.5} \qquad (1)$$

which is consistent with the results[14] for an asymmetric configuration similar to our experiment. Using a powered electrode diameter of 12.7 cm and a grounded electrode diameter of approximately 17.78 cm, the theoretical model (1) is compared with the measured potential $V_{\rm p}$ in Fig.5. There is good agreement between the measurements and calculations.

The density from the Langmuir probe measurements can also be compared with a density estimated indirectly from power balance considerations. For the asymmetric confined discharge this is approximated using the formula at pp408–413 in Ref.[12] as

$$n = P_{\rm abs}/eh_l u_{\rm B}[A_{\rm tot}(\varepsilon_{\rm c} + 2T_{\rm e}) + 0.78A_{\rm a}V_{\rm a} + 0.78(A_{\rm tot} - A_{\rm b})V_{\rm p}] \quad (2)$$

where

$$A_{\rm tot} = 2\pi R_{\rm b}^2 + 2\pi R_{\rm b} l$$

is the total loss area of the discharge,

$$h_l = 0.86/(3 + l/2\lambda_{\rm i})^{1/2} \quad (3)$$

the edge-to-centre density ratio in the main discharge determined from diffusion theory, $\lambda_{\rm i}$ the ion-neutral mean free path, $u_{\rm B} = (eT_e/M)^{1/2}$ the Bohm speed, and $\varepsilon_{\rm c}$ the collisional energy loss per electron–ion pair created in the discharge. For argon, $\lambda_{\rm i} \approx 1/33\ p$ (in units of m), with p being the pressure in mTorr, and $\varepsilon_{\rm c}$ is obtained from p82 in Ref.[12]. A comparison between the values is given in Table 1 at 100 mTorr where the electron temperature $T_{\rm e} \approx 2.1$ V and $\varepsilon_{\rm c} \approx 116$ V. From the above comparisons, we see that the stable confined plasma is well-characterized theoretically.

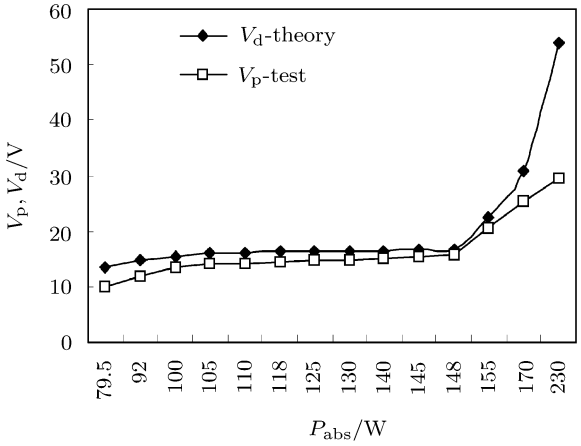


Fig.5. Theoretical and measured potential.

Table 1. Comparison between central plasma density n measured with the Langmuir probe and the density calculated from power balance.

$P_{\rm abs}$/W	$V_{\rm rf}$(p-p)/V	$V_{\rm a}$(p-p)/V	$V_{\rm p}$(p-p)/V	$n_{\rm calculated}/{\rm cm}^{-3}$	$n_{\rm measured}/{\rm cm}^{-3}$
20	116	98	18	5.10×10^{10}	6.42×10^{10}
40	150	126	24	9.91×10^{10}	1.04×10^{11}
55	190	160	30	1.32×10^{11}	1.38×10^{11}
85	225	189	36	1.98×10^{11}	2.41×10^{11}
95	247	208	39	2.18×10^{11}	2.91×10^{11}

Note that pressure is 100 mTorr.

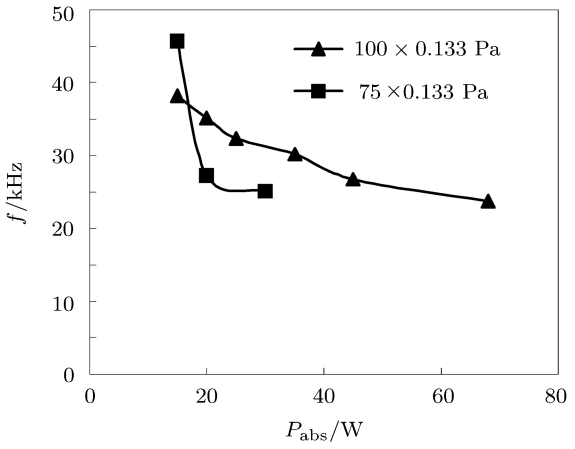


Fig.6. Oscillation frequency of optical emission versus power in a high-frequency range.

The oscillation frequencies ranging from 0 to tens of kHz and from 0 to several Hz varying with the absorbed power at a constant pressure are shown in Figs.6 and 7 respectively. The frequency in the case of high-frequency oscillation decreases as the power increases, roughly proportional to $1/P_{\rm abs}$, while the frequency in the case of low-frequency oscillation has a maximum with respect to the absorbed power. At a constant power, the frequency in the case of high-frequency oscillation increases with pressure increasing as shown in Fig.8. The reason for these variations is not clear at present.

The theory of high-frequency relaxation oscillations was developed in Ref.[2]. It has been shown that the ignition of slot plasma causes the main plasma voltage $V_{\rm p}$ to drop off due to an increase in the grounded area seen by the main discharge. This will extinguish the slot discharge but may leave the main discharge ignited. However, the additional detuning of the match and the overall lowering of the value of circuit quality factor Q both can extinguish the main

discharge. Because the formation of a slot plasma results in the propagation of a surface wave with a significant phase shift and resistive decay, an electromagnetic analysis in the slot is required. Hence, the high-frequency oscillations are essentially understood as an instability induced by an increase in resistance and capacitance of the discharge when the slot plasma ignites. A particular tuning of the matching network investigated, both experimentally and theoretically, indicates that the transient ignition of the slot plasma increases the capacitance of the plasma to ground and lowers the system Q value at the expense of losing the overall equilibrium. This causes the voltage across the discharge to drop off dramatically, and in consequence the electron temperature decreases. The main discharge density correspondingly decays but at a slower rate, until the faster decay of the slot plasma density re-ignites the discharge, therefore, the above scenario will be repeated. The oscillation frequency as well as the shapes of the light emission signal and plasma density, obtained from the model, agrees reasonably well with the corresponding experimental observations.

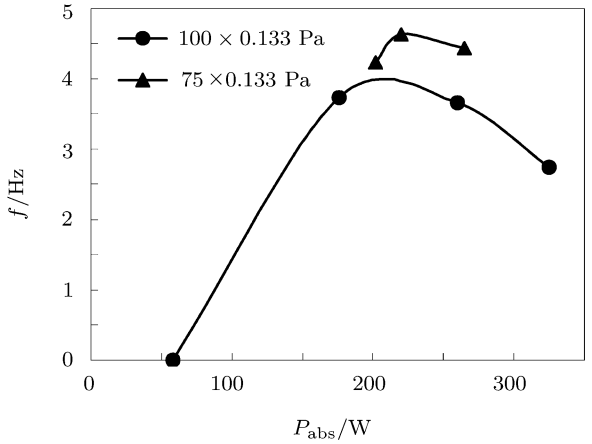


Fig.7. Oscillation frequency versus power in a low-frequency range.

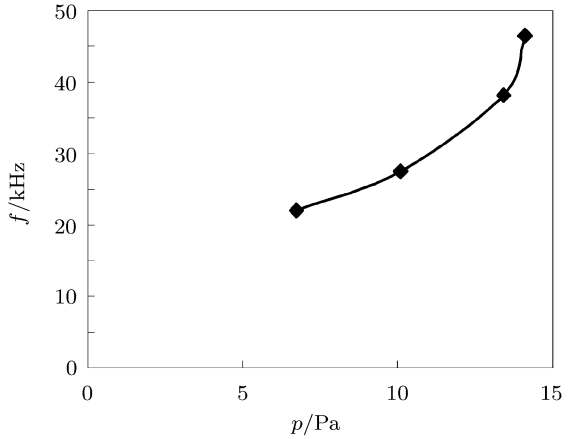


Fig.8. Oscillation frequency versus pressure in a high-frequency range and at power = 15 W.

Although a systematic study of the behaviour as a function of the degree of matching is not undertaken, some behaviours are found experimentally, and seen theoretically in the model. These include frequencies in a kHz range, similar to those observed experimentally, and also instability conditions in which the main plasma is not fully extinguished.

3. Oscillations in inductive reactors

The experimental setup[5,7] is a transformer coupled plasma (TCP) source as schematically shown in Fig.2. The plasma is generated in a cylindrical aluminium vacuum chamber which is 305 mm in diameter and is 215 mm long. A quartz window is mounted at each end of the chamber. The right-hand window is 19.05 mm thick and placed on an aluminium flange with a 185 mm diameter opening.

The gas flowing into the chamber is argon (0–100 standard cc/minute (sccm)), or oxygen (0–100 sccm), or sulfur hexafluoride (0–100 sccm), each is controlled by a mass flow controller. The pressure in the chamber is monitored with a capacitive manometer. The gas pressure can be adjusted manually by changing the opening of the gate valve and can be varied in a range of 0.067–39.9 Pa. The gas is pumped by a 340 l/s turbomolecular pump backed by a rotary pump giving a base pressure of about 0.133×10^{-6} Pa.

A three-turn planar spiral coil placed on the right quartz window as shown in Fig.2 generates the rf electromagnetic field to create and sustain the plasma in the chamber. The coil is made up of 8 mm diameter copper tube and has an outer diameter of 175 mm and a 3 cm spacing between the turns, supported by a Teflon holder. The coil is cooled using a closed-loop deionized water system with temperature and pressure control. The coil is powered by a 2 kW power supply at 13.56 MHz through a conventional L-type

matching network.

The experimental setup has diagnostics to measure the parameters of the plasma in the stable and unstable modes of operation and the external electrical characteristic quantities of the plasma system. The diagnostics include optical emission and mass spectroscopy, movable electrostatic probes immersed in the plasma, and rf power, voltage, and current meters for the external circuit. Two optical emission spectroscopic systems detect the light emitted from the bulk plasma, argon emission (748.7 nm) or fluorine emission (703.7 nm) lines, as a function of time. One optical emission spectroscopy (OES) system is equipped with a monochromator, the other one uses optical filters for argon and fluorine emission lines. A VG quadrupole mass spectrometer is used. Two movable electrostatic probes are used to measure the charged particle densities in both stable and unstable plasma regimes. A small cylindrical Langmuir probe made of a 0.13 mm diameter and 5 mm long platinum wire biased at a constant voltage is used to measure the time variations of the electron current and floating potential in the unstable plasma.

An example of such instabilities in a 0.66 Pa Ar/SF_6 (1:1) mixture at a 550 W discharge power with 13.56 MHz is shown in Fig.9 where the traces of the positive ion and electron densities measured with Langmuir probes and the negative ion density obtained by subtraction are plotted as a function of time. The frequency of instability is usually in a range from 0 to a few kHz.

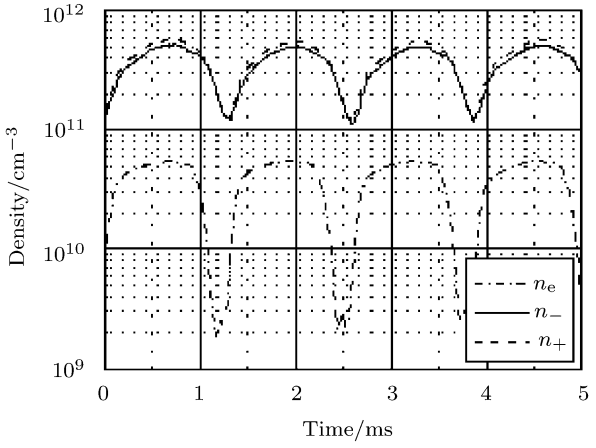


Fig.9. Positive ion, negative ion and electron densities as a function of time in a 0.67 Pa Ar/SF_6 (1:1) mixture at 550 W with 13.56 MHz.

The regions of instability in pure SF_6 and Ar/SF_6 (1:1) mixture are shown in Figs.10(a) and 10(b), respectively. In both cases, the matching network is tuned just below the unstable region in the stable capacitive mode to obtain a minimum of reflected power, and further varied as the rf power increases correspondingly, the discharge runs through the unstable regime and then into the inductive regime. In order to keep reflected power lower the matching network should be carefully adjusted to work in an optimal condition. Instabilities exist in the whole range of pressures from 0.266 to 13.33 Pa. In the pure SF_6 plasma, the window of instability is larger than in the Ar/SF_6 mixture; increasing the argon partial pressure in the mixture can narrow the window.

The frequency of the instability as a function of rf power for different pressures of pure SF_6 discharge is shown in Fig.11. In these experiments, the matching network was set to minimize the reflected power at each point of the measurements. The instability frequencies are plotted for pressures from 1.33 to 13.33 Pa. For these higher pressures, the instability frequency increases with the power increase, and for the pressures above 2.66 Pa, there are an almost linear dependence of the frequency on the discharge power, and a square root dependence on pressure, in a range of frequencies from 20 to 100 kHz. At higher pressures, the oscillations of light have small modulations compared with those at lower pressures where the light signal oscillates between a maximum and a minimum that is close to zero.

A volume averaged (global) model for the kilohertz instability is developed in Refs.[4–7]. The model assumes a low-pressure discharge with a large number of negative ions. In order to calculate the volume effects, the densities are taken as being uniform within the bulk plasma. The surface losses are calculated from a parabolic distribution of positive and negative ions assuming that the discharge does not have an electropositive edge region. The electrons and negative ions are assumed to be in Boltzmann equilibrium. The ion temperatures are taken as being constant, with positive ions being at room temperature and negative ions being at $T_- = 0.3$ eV. During the instability, the electron density, ion densities and electron temperature T_e are all time-varying quantities. The neutral and excited neutral gas densities are assumed to be constant.

The physics of the instability depends on the difference in time scale between electron and ion dynamics as explained below. At low negative ion densities the positive ion and electron densities build up till a

stable high-density inductive equilibrium occurs. The negative ion density builds up on a slower time scale, increasing the electron loss. When the loss is sufficiently high the inductive equilibrium can no longer be maintained. Then the discharge, thus the electron density collapses to a capacitive equilibrium. Again, on a slower time scale, the negative and positive ion densities decay, primarily by recombination, until the losses fall to the level at which the inductive equilibrium can be established again, resulting in a relaxation oscillation. The instability occurs in a power window, because at higher powers the inductive mode can be maintained against all losses, while at lower powers only a capacitive mode can exist.

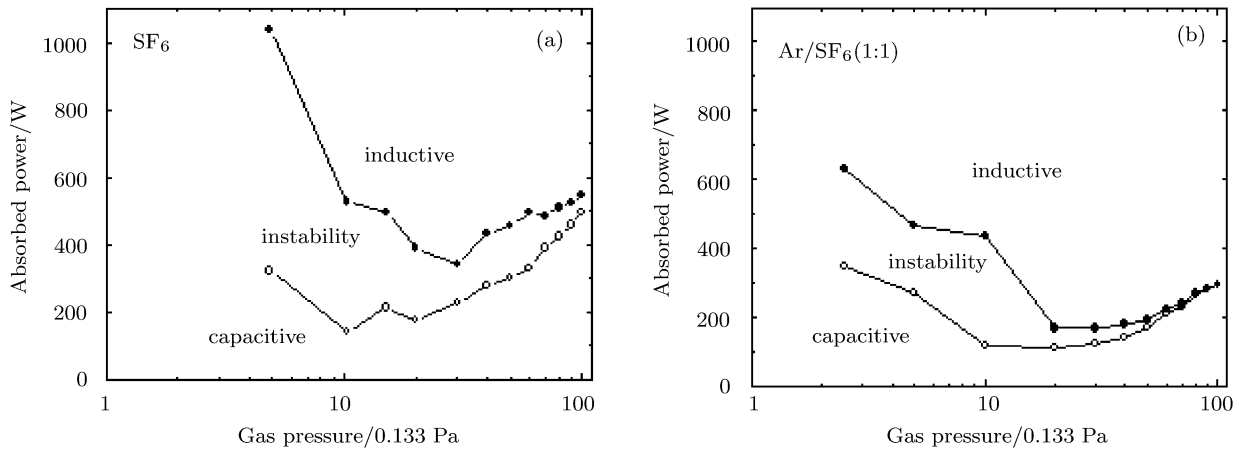


Fig.10. Windows of instability in (a) pure SF_6 and (b) Ar/SF_6 (1:1) mixture plasmas.

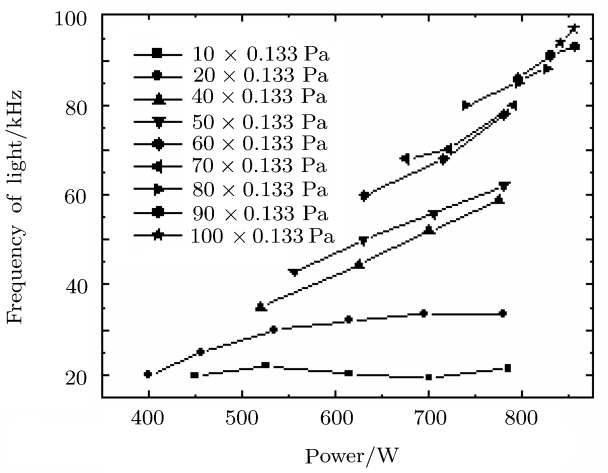


Fig.11. Oscillation frequency of instability as a function of rf power in pure SF_6 plasma for pressures above 1.33 Pa.

4. Conclusions and further discussion

Both electropositive capacitive discharges and electronegative inductive discharges are found experimentally to exhibit high (kilohertz) and low (hertz) frequency relaxation oscillations due to instabilities. For the kilohertz oscillations in a capacitive reactor, in which the main discharge is connected to a grounded peripheral region through a dielectric slot, ignition of slot plasma causes the main plasma voltage to drop off due to an increase in the grounded area seen by the main discharge. This extinguishes the slot discharge but may leave the main discharge ignited. However, additional detuning of the match and an overall lowering of the circuit Q value result also in extinguishing the main discharge. This causes the voltage across the discharge to drop off dramatically, causing the electron temperature to decrease also. The main discharge density correspondingly decays but at a slower rate, until the faster decay of the slot plasma density re-ignites the discharge, repeating the scenario.

For the kilohertz oscillations in low-pressure inductive discharges, it is found experimentally that the discharge is unstable in the transition from a low density capacitive to a high density inductive mode of operation, when attaching gases such as SF_6 or Ar/SF_6 mixtures are used such that the plasma contains negative ions. The size of unstable region in power can

be varied by changing the discharge pressure, gas flow rate, and chemical composition of the plasma. An increase of the argon partial pressure in Ar/SF_6 mixture reduces the average attachment rate of the negative ions and narrows the instability window, which finally disappears in pure argon discharge.

Most of these phenomena and their parameter scaling can be qualitatively understood from a volume-averaged (global) model for the instability in an electronegative gas discharge. Power and positive and negative particle density balance differential equations are used to produce the dynamic behaviours. An equivalent circuit model with a matching network and capacitive and inductive coupling branches is used to define the energy deposition in the discharge.

The kilohertz relaxation oscillations in capacitive reactors, which depend nonlinearly on two states existing for the discharge, have a resemblance to those in electronegative inductive reactors. In the latter case there is a separation of timescales between the electrons and negative ions that control the frequency and amplitude of the instability, with the slowest timescale for decay of the negative ion density essentially controlling the oscillation frequency. For the capacitive reactor, there is also a separation of timescales, with an assumed fast ionization time for the ignition of the slot plasma, and with the slower timescale for plasma decay in the slot controlling the oscillation frequency. In both situations, the matching network dynamics has been found to play an important role in the instability dynamics.

In contrast to the kilohertz oscillations, the unstable oscillations at hertz frequencies in both capacitive and inductive reactors have been reasonably well-characterized experimentally, but an adequate theoretical understanding of the phenomena has not been developed yet.

Acknowledgments

The authors wish to thank Professor A. J. Lichtenberg for many useful discussions and suggestions. They acknowledge the support provided by the Lam Research Corporation, the State of California MICRO Program, National Science Foundation (Grant No ECS-0139956), and a University of California Discovery (Grant from the Industry-University Cooperative Research Program (IUCRP).

Professor Zhou Zhu-Wen performed this work as a visiting scholar in the Department of Electrical Engineering and Computer Sciences, University of California at Berkeley from May 2005 to May 2006.

References

[1] Lieberman M A, Lichtenberg A J, Kim S, Gudmundsson J T, Keil D L and Kim J 2006 *Plasma Sources Sci. Technol.* **15** 276

[2] Zhou Z W, Lieberman M A and Kim S 2006 *Chin. Phys. Lett.* **23** 2251

[3] Tuszewski M 1996 *J. Appl. Phys. Lett.* **79** 8967

[4] Lieberman M A, Lichtenberg A J and Marakhtanov A M 1999 *Appl. Phys. Lett.* **75** 3617

[5] Chabert P, Lichtenberg A J, Lieberman M A and Marakhtanov A M 2001 *Plasma Sources Sci. Technol.* **10** 478

[6] Lichtenberg A J, Chabert P, Lieberman M A and Marakhtanov A M in 2001 *Bifurcation Phenomena in Plasmas* (Fuhuoka: Kyushu University)

[7] Marakhtonov A M, Tuszewski M, Lieberman M A, Lichtenberg A J and Chabert P 2003 *J. Vac. Sci. Technol.* A **21** 1849

[8] Chabert P, Abada H, Booth J P and Lieberman M A 2003 *J. Appl. Phys.* **21** 8979

[9] Corr C S, Steen P G and Graham W G 2003 *Plasma Sources Sci. Technol.* **12** 265

[10] Lieberman M A and Gottscho R A 1994 in *Physics of Thin Films for Thin Film Deposition and Etching* (New York: Academic) Vol. 18

[11] Tsai W, Mueller G, Lindquist R, Frazier B and Vahedi V 1996 *J. Vac. Sci. Technol.* B **14** 3276

[12] Lieberman M A and Lichtenberg A J 2005 *Principles of Plasma Discharges and Materials Processing* (New York: Wiley)

[13] Gudmundsson J T and Lieberman M A 1998 *Plasma Sources Sci. Technol.* **7** 1

[14] Lieberman M A and Savas S E 1990 *J. Vac. Sci. Technol.* A **8** 1632